# Variability of sulfate signal in ice-core records based on five replicate cores

Gautier Elsa[1, 2], Savarino Joël[1, 2], Erbland Joseph[1,2], Lanciki Alyson[1,2], Possenti Philippe[1,2]

[1]Univ. Grenoble Alpes, LGGE, F-38000 Grenoble, France

[2]CNRS, LGGE, F-38000 Grenoble, France

## Abstract

Current volcanic reconstructions based on ice core analysis have significantly improved over the past few decades by incorporating multiple core analysis with high temporal resolution from different parts of the polar regions. Regional patterns of volcanic deposition are based on composite records, built from cores taken at both poles. However, in many cases only a single record at a given site is used for these reconstructions. This assumes that transport and regional meteorological patterns are the only source of the dispersion of the volcanic-products. Here we evaluate the local scale variability of a sulfate profile in a low accumulation site (Dome C, Antarctica), in order to assess the representativeness of one core for such reconstruction. We evaluate the variability with depth, statistical occurrence, and sulfate flux deposition variability of volcanic eruptions detected on 5 ice cores, drilled 1 meter away from each other. Local scale variability, essentially attributed to snow drift and surface roughness at Dome C, can lead to a non-exhaustive record of volcanic events when a single core is used as the site reference with a bulk probability of 30 % of missing volcanic events and close to 65 % uncertainty on one volcanic flux measurement (based on the standard deviation obtained from a 5 cores comparison). Averaging n records reduces significantly (by a factor $1/\sqrt{n}$) the uncertainty of the deposited flux mean; in the case of 5 cores, the uncertainty of the mean flux can therefore be reduced to 29%.

## Introduction

When a large and powerful volcanic eruption occurs, the energy of the blast is sufficient to inject megatons of material directly into the upper atmosphere [*Robock*, 2000]. While ashes and pyroclastic materials fall rapidly to the ground because of gravity, gases remain over longer time scales. Among gases, $SO_2$ is of a particular interest due to its conversion to tiny sulfuric acid aerosols, which can potentially impact the radiative budget of the atmosphere [*Rampino and Self*, 1982; *Timmreck*, 2012]. In the troposphere a combination of turbulence, cloud formation, rainout and downward transport are efficient processes that clean the atmosphere of sulfuric acid, and volcanic sulfuric acid layers rarely survive more than a few weeks, limiting their impact on climate. The story is different when volcanic $SO_2$ is injected into the stratosphere. There, the dry, cold and stratified atmosphere allows sulfuric acid layers to remain for years, slowly spreading an aerosol blanket around the globe. The tiny aerosols then act as efficient reflectors and absorbers of incoming solar radiations, significantly modifying the energy balance of the atmosphere [*Kiehl and Briegleb*, 1993] and the ocean [*Gleckler et al.*, 2006; *Miller et al.*, 2012; *Ortega et al.*, 2015]. With a lifetime of 2 to 4 years, these aerosols of sulfuric acid ultimately fall into the troposphere where they are removed within weeks.

In Polar Regions, the deposition of the sulfuric acid particles on pristine snow will generate an acidic snow layer, enriched in sulfate. The continuous falling of snow, the absence of melting and the ice thickness make the polar snowpack the best records of the Earth's volcanic eruptions. *Hammer* [1977] was the first to recognize the polar ice propensity to record such volcanic history. Built on the seminal work of Hammer et al., a paleo-volcanism science developed around this discovery with two aims.

The first relies on the idea that the ice record can reveal past volcanic activity and, to a greater extent, its impact on Earth's climate history [*Robock*, 2000; *Timmreck*, 2012]. Indeed, at millennium time scale, volcanoes and the solar activity are the two main recognised natural climate forcings [*Stocker et al.*, 2013]. Based on ice records, many attempts are made to extract the climate forcing induced by a volcanic eruption [*Crowley and Unterman*, 2013 ; *Gao et al*., 2008; *Gao et al*., 2007; *Sigl et al*., 2013; *Sigl et al*., 2014; *Zielinski*, 1995]. However, such an approach is inevitably prone to large uncertainty

53 pertaining to the quality of the ice record and non-linear effects between deposition fluxes and source
54 emissions [*Pfeiffer et al.*, 2006].
55 The second aim of the paleo-volcanism is to provide an absolute dating scale when clear volcanic
56 events in differently located ice cores can be unambiguously attributed to the same dated event [*Severi*
57 *et al.*, 2007]. The time synchronization of different proxy records is possible, allowing study of the
58 phasing response of different environmental parameters to climate perturbation [*Ortega et al.*, 2015;
59 *Sigl et al.*, 2015] or estimating the snow deposition over time [*Parrenin et al.*, 2007]. Whatever the
60 intent, paleo-volcanism should rely on robust and statistically relevant ice core records.
61 Work to establish a volcanic index, undertaken to date, has assumed volcanic events are clearly
62 identified, without any false signal from background variations induced by other sulfur sources (eg
63 marine, anthropogenic, etc.). Seasonal layer counting is used whenever possible, bi-polar comparison
64 of ice sulfate records has become the method of choice to establish an absolute dated volcanic index
65 [*Langway et al.*, 1988]. Both known and unknown events can be used to synchronize different cores.
66 However, only a limited number of peaks, with characteristic shape or intensity, and known to be
67 associated with a dated eruption, can be used to set a reliable time scale [*Parrenin et al.*, 2007]. This
68 restriction is partly fueled by the poor and/or unknown representativeness of most volcanic events
69 found in ice cores. Most of the time, a single core is drilled at a given site and used for cross
70 comparison with other sites. This approach is clearly insufficient for ambiguous events.
71 At a large scale, sulfate deposition is highly variable in space and mainly associated with atmospheric
72 transport and precipitation patterns. At a local scale (ca. 1m), variability can emerge from post-
73 deposition processes. While sulfate is a non-volatile species supposed to be well preserved in snow,
74 spatial variability is induced by drifted snow, wind erosion leading to surface roughness
75 heterogeneities [*Libois et al.*, 2014]. These effects are amplified in low accumulation sites where most
76 of the deep drilling sites are performed [*EPICA-community-members*, 2004; *Jouzel*, 2013; *Lorius et al.*,
77 1985]). To the best of our knowledge, one single study has used multiple drillings at a given site to
78 analyze the representativeness of the ice core record [*Wolff et al.*, 2005]. This study took advantage of
79 the two EPICA cores drilled at Dome C, 10 m apart (Antarctica, 75°06'S, 123°21'E, elevation 3220 m,

mean annual temperature -54.5°C) [*EPICA-community-members*, 2004] to compare the dielectric profile (DEP) along the 788 m common length of the two cores. For the two replicate cores, statistical analysis showed that up to 50 % variability in the pattern of any given peak was encountered as a consequence of the spatial variability of the snow deposition. The authors concluded that ice-core volcanic indices from single cores at such low-accumulation sites couldn't be reliable and what was required was a network of close-spaced records. However, as mentioned in Wolff's conclusion, this statistical study relied only on two records. Additionally, DEP signals are known to be less sensitive than sulfate signals for volcanic identification, and more accuracy is expected by comparing sulfate profiles. The authors thus encouraged conducting a similar study on multiple ice cores to see if the uncertainty could be reduced.

In the present study we took advantage of the drilling of 5 ice cores at Dome C, initially intended for the analysis of sulfur isotopes of the volcanic sulfate. Putting aside the number of records, our approach is similar in many points to Wolff's work. However, it has the advantage of relying on highly resolved sulfate profiles. In addition, the spatial scale is slightly smaller as the 5 cores were drilled 1-meter apart. The comparison of 5 identically processed cores is a chance to approach the representativeness of a single core reconstruction at a low accumulation site, the most prone to spatial variability. The representativeness of a volcanic record can be assessed by isolating the volcanic peaks in different records, as done in Wolff's work and in this study, or by a global comparison of the sulfate concentration records as proposed in Gfeller et al. (2014). In the later case, the full individual profiles (background + the volcanic peaks) are compared to a theoretical ideal case made of an infinite number of profiles. A similarity coefficient is then calculated between a population made of n profiles and the infinite population. However, this approach can't be extrapolated to discret profiles, as in our approach, because there is a priori no ideal profile for the volcanic record. Nevertheless, the representativeness of sulfate in Dome C record, as defined by Gfeller et al. work, has been also calculated for element of comparison with this method, and the result is available in the supplementary online material (fig. S1).

New constraints on variability of sulfate deposition recorded by spatial heterogeneity in such sites are

expected from the present work. Even if recent publications [Sigl et al., 2014], underline the need of using multiple records in low accumulation sites, to overcome the spatial variability issue, such records are not always available. This lack of records adds uncertainty in the volcanic flux reconstruction based on polar depositional pattern. Our study should help to better constrain the error associated with local scale variability, and ultimately, the statistical significance of volcanic reconstructions. The present study discusses the depth shift, occurrence of events and deposition flux variability observed in the 5 cores drilled.

## Experimental setup and Methods

### Core drilling

The project "VolSol", initiated in 2009, aimed at constraining the estimation of the natural part of radiative forcing, composed of both volcanic and solar contributions using ice core records of sulfate and $^{10}$Be. In order to build a robust volcanic index including a discrimination of stratospheric events based on sulfur isotopic ratios [*Baroni et al.*, 2008; *Savarino et al.*, 2003], 5 x 100 m-firn cores (dia. 10 cm) were drilled in 2010/2011 along a 5 m straight line, and spaced approximately 1 m apart. The drilling took place at the French-Italian station Concordia, more precisely between Concordia station and EDC drilling tent (300m west of the EDC drilling tent). At this site, the mean annual snow accumulation rate is about 25 kg $m^{-2}$ $y^{-1}$, leading to an estimated time-period covered by the cores of 2500 years. Cores were logged and bagged in the field, and temporarily stored in the underground core buffer (- 50 °C) before analysis. The unusual number of ice core drilled at the same place was driven by the amount of sulfate necessary to conduct the isotopic analysis. However, this number of replicate cores drilled 1m apart offers the opportunity to question the representativeness of a volcanic signal extracted from a single core per site.

### Sampling, Resolution and IC Analyses

Analyses were directly performed in the field during two consecutive summer campaigns. Thirty

meters were analyzed in 2011, the rest was processed the following year. The protocol was identical for each core and the steps followed were:

- Decontamination of the external layer by scalpel scrapping
- Longitudinal cut with a band saw of a 2 cm stick of the most external layer
- Sampling of the ice stick at a 2 cm-resolution (ca. 23 600 samples)
- Thawing the samples in 50 ml centrifuge tubes, and transfer in 15 ml centrifuge tubes positioned in an autosampler
- Automatic analysis with a Metrohm IC 850 in suppressed mode (NaOH at 7 mM, suppressor $H_2SO_4$ at 50 mM, Dionex AG11 column), in a fast IC configuration (2 min run) with regular calibration (every 60 samples) using certified sulfate reference solution (Fisher brand, 1000 ppm certified).

Due to the fragility of snow cores, the first 4 m were only analyzed on a single core (Figure 1). We will thus not discuss the variability of the Pinatubo and Agung eruptions present in these first 4 meters. Concentration data are deposited in the public domain and made freely available in NOAA National Climatic Data center.

**Peaks discrimination method**

As with most algorithms used for peak detection, the principle is to detect anomalous sulfate concentration peaks from a background noise (stationary or not), which could potentially indicate a volcanic event. The estimation of the background value should therefore be as accurate as possible. Using core 2 as our reference core, we observed a background average value stationary and close to 85 ppb ± 30 ppb (1σ) at Dome C during the 2,500 years of the record. However, the variability is sufficient enough to induce potential confusion on detection of small peaks. Therefore, a stringent algorithm using PYTHON language (accessible on demand) was developed to isolate each possible peak. The algorithm treats the full ice record by 1-meter section (ca. 45-50 samples). For each meter, a mean concentration (m) and standard deviation (σ) is calculated regardless of the presence or not of peaks in the section. Then, every value above the $m + 2\sigma$ is removed from the 1-meter dataset. A new mean and standard deviation is calculated and the same filtration is applied. Iteration runs until no

more data above m + 2 σ is found. At that point, m represents the background mean concentration (The resulting background estimation along core 1 is illustrated in SOM, figure S2). The process runs for each 1-m section, starting from the surface sample and until the end of the core. Then, each 1-meter dataset is shifted by one sample; the process is reset and the peak detection run again on each new 1-m dataset. Sample shift is applied until the last sample of the first 1-meter section is reached so that no bias is introduced by the sampling scheme. Every concentration data point is thus compared approximately with its 100 neighboring data (50 of each side). Each data point isolated by the algorithm is further tested. To be considered as a point belonging to a potential volcanic peak, the data should be detected in a given core (i.e. for being above the m + 2 σ final threshold) in at least 50 % of the 50 runs. Additionally, the point has to be part of at least three consecutive points passing the same 50 % threshold detection. This algorithm was applied individually on each core, giving 5 different lists of peak. In total, 54, 51, 47, 50 and 47 peaks were detected on core 1, 2, 3, 4 and 5, respectively. A manual detection is then required if one wants to build a more accomplished volcanic record from several profiles, which must be based on shape criteria, and not only statistical criteria. However, in the scope of this paper, no manual sorting was applied, so that the statistical assessment could rely on more objective criteria (the number of occurrences).

**Core synchronization and dating**

Core 1 was entirely dated with respect to the recently published volcanic ice core database [*Sigl et al.*, 2015] using *Analyseries* 2.0.8 software (http://www.lsce.ipsl.fr/Phocea/Page/index.php?id=3), and covers the time period of -588 to 2010 CE. Figure 2 shows the age-depth profile obtained for this core. A total of 13 major volcanic eruptions well dated were used as time markers to set a time scale (bold date in Table 1). Core 1 was entirely dated through linear interpolation between those tie points. Dated core 1 was then used as a reference to synchronize the remaining 4 cores, using the same tie points and 10 additional peaks (non-bold date in Table 1), presenting characteristic patterns common to each core. In total, 23 points were therefore used to synchronize the cores.

### Composite building from the 5 ice cores

Through the routine described above, the five cores are depth-synchronized using the 23 tie points and other potential volcanic events in each core cores are detected independently. Therefore, the number of peaks detected in each core is different (between 47 and 54) and their depth (with the exception of the tie points used) is slightly different to each other cores due to sampling scheme and position of the maximum concentration. After correcting the depth shift between cores, a composite profile was built by summing all the peaks identified in the 5 cores. In this composite, sulfate peaks from different cores are associated to a same event as soon as their respective depth (corresponding to the maximum concentration) are included in a 20cm depth window. This level of tolerance is consistent with the dispersion in width and shape of peaks observed (Figure 3). A number of occurrences is then attributed to each sulfate peak, reflecting the number of times it has been detected in the 5 cores dataset (Figure 4).

## Results and Discussions

### Depth offset between cores

Depth offsets between cores are the result of the surface roughness at the time of drilling, variability in snow accumulation, heterogeneous compaction during the burying of snow layers and logging uncertainty. This aspect has been discussed previously, over a similar time-scale (Wolff et al. 2005), and over a longer time-scale (Barnes et al. 2006) in Dome C. Surface roughness, attributed to wind speed, temperatures and accumulation rate, is highly variable in time and space. These small features hardly contribute to the depth offset on a larger spatial scale, in which case glacial flow can control the offset between synchronized peaks, as it seems to be the case in South Pole site (Bay et al. 2010). However, in Dome C, and at the very local spatial scale we are considering in the present work, roughness is significant regarding to the accumulation rate. It is therefore expected that synchronized peaks should be found at different depths. The offset trend fluctuates with depth, due to a variable

212 wind speed (Barnes et al. 2006). To estimate the variability in the depth shift for identical volcanic
213 events, we used the tie points listed in Table 1. For each peak maximum, we evaluate the depth offset
214 of core 1, 3, 4 and 5, with respect to core 2. To avoid logging uncertainty due to poor snow
215 compaction in the first meters of the cores and surface roughness at the time of the drilling, we used
216 the UE 1809 depth in core 2 (13.30 m) as a depth reference horizon from which all other depth cores
217 were anchored using the same 1809 event. For this reason, only eruptions prior to 1809 were used to
218 evaluate the offset variability, that is 18 eruptions instead of the 23 used for the core synchronization.
219 Figure 5, shows the distribution of depth shift of the cores with respect to core 2. While the first 40 m
220 appear to be stochastic in nature, a feature consistent with the random local accumulation variations
221 associated with snow drift in Dome C site, it is surprising that at greater depth, offset increases (note
222 that the positive or negative trends are purely arbitrary and depends only on the reference used, here
223 core 2). The maximum offset, obtained between core 3 and 5 is about 40 cm. Such accrued offsets
224 with depth were also observed by *Wolff et al.*, [2005] and were attributed to the process of logging
225 despite the stringent guidelines used during EPICA drilling. Similarly, discontinuities in the depth
226 offset, observed by *Barnes et al.,* [2006] were interpreted as resulting from logging errors. As no
227 physical processes can explain a trend in the offsets, we should also admit that the accrued offset is
228 certainly the result of the logging process. In the field, different operators were involved but a
229 common procedure was used for the logging. Two successive cores extracted from the drill were
230 reassembled on a bench to match the non uniform drill cut and then hand sawed meter by meter to get
231 the best precise depth core, as neither the drill depth recorder nor the length of the drilled core section
232 can be used for establishing the depth scale. This methodology involving different operators should
233 have randomized systematic errors but obviously this was not the case. Despite the systematic depth
234 offset observed, synchronization did not pose fundamental issues as the maximum offset in rescaled
235 profiles never exceeds the peak width (ca. 20 cm) thank to the 10 possible comparisons when pair of
236 core are compared. Confusion of events or missing of events are thus very limited in our analysis (see
237 next section).
238

**Variability in events occurrence**

The variability in events occurrence in the 5 ice cores has been evaluated through the construction of a composite record (Figure 4) and the counting of events in each core as described in the method. By combining the five ice cores, we listed a total amount of 91 sulfate peaks (Pinatubo and Agung not included), which are not necessarily from volcanic sources. Some peaks can be due to post deposition effects affecting the background deposition, or even contamination. When it comes to defining a robust volcanic index, peak detection issues emerge. Chances to misinterpret a sulfate peak and assign it, by mistake, to a volcanic eruption, as well as chances to miss a volcanic peak, can be discussed through a statistic analysis conducted on our five cores.

We try to evaluate to what extent multiple cores comparison facilitates the identification of volcanic peaks, among all sulfate peaks that can be detected in a core. To do so, we assumed that a peak is of volcanic origin as soon as it is detected at least in two cores. In other words, the probability to have two non-volcanic peaks synchronized in two different cores is nil. It is expected that combining an increasing number of cores will increasingly reveal the real pattern of the volcanic events. All possible combinations from 2 to 5 cores comparison were analyzed, totalizing 26 possibilities for the entire population. The results for each comparison were averaged, giving a statistic on the average number of volcanic peaks identified per number of cores compared. The results of the statistical analysis are presented in Figure 6. As expected, in a composite made of 1 to 5 cores, the number of sulfate peaks identified as volcanic peaks (for being detected at least twice) increases with the number of cores combined in the composite. Thus, while only 30 peaks can be identified as volcanic from a two cores study, a study based on 5 cores can yields 62 such peaks. The 5-cores comparison results in the composite profile given in Figure 4a. The initial composite of 93 peaks is reduced to 64 volcanic peaks (Pinatubo and Agung included) after removing the single peaks (Figure 4b). Each characteristic of the retained peaks is given in Table 2. The main conclusion observing the final composite record is that only 17 of the 64 peaks were detected in all of the 5 cores and 68 % of all peaks were at least present in two cores. At the other side of the spectrum, 2-cores analysis reveals that only 33 % (30 peaks on average) of the peaks are identified as possible eruptions. Two cores comparison presents

still a high risk of not extracting the most robust volcanic profile at low accumulation sites, a conclusion similar to *Wolff et al.*, [2005]. Surprisingly, it can also be noticed that this 5-core comparison doesn't results in an asymptotic ratio of identified volcanic peaks, suggesting that 5 cores are not sufficient either to produce a full picture. High accumulation sites should be prone to less uncertainty; however, this conclusion remains an a priori that still requires a confirmation.

Large and small events are not equally concerned by those statistics. Figure 7 shows that the probability of presence is highly dependent on peak flux and the chance to miss a small peak (maximum flux in the window $[f + 2\sigma : f + 5\sigma]$, f being the background average flux) is much higher than the chance to miss a large one (maximum flux above $f + 8\sigma$). However, it is worth noticing that major eruptions can also be missing from the record, as it has already been observed in other studies [*Castellano et al.*, 2005; *Delmas et al.*, 1992]. The most obvious example in our case is the Tambora peak (1815 AD), absent in 2 of our 5 drillings, while presenting an intermediate to strong signal in the others (Figure 8). The reason for the variability in event occurrence has been discussed already by *Castellano et al.*, [2005]. In the present case of close drillings, long-range transport and large-scale meteorological conditions can be disregarded due to the small spatial scale of our study; the snow drift and surface roughness is certainly the main reasons for missing peaks. The fact that two close events as UE 1809 and Tambora are so differently recorded indicates that post-depositional effects can affect the recording of eruptions very variably in time and space.

**Variability in signal strength**

To compare peak height variability, detected peaks were corrected by subtracting the background from peak maxima. We considered $C_i/C_{mean}$ variations, $C_i$ being the $SO_4^{2-}$ maximum concentration in core i (1 to 5), and $C_{mean}$ being the mean of those concentrations for the event i. Ci is considered nil if the peak is not detected in a core. For concentration values, positive by definition, the log-normal distribution is more appropriate; geometric means and geometric standard deviations were used, as described by *Wolff et al.*, [2005] (Table 3). In our calculation, the geometric standard deviation based on 5 cores is 1.49; in other words, the maximum concentration of a peak in one core is uncertain by

293 49%. This factor is completely in agreement with the one obtained in *Wolff et al.*, [2005] (1.5). Having
294 n cores allows for a reduction of the uncertainty on the mean (standard error of the mean) by a factor
295 $1/\sqrt{n}$. The peak heights mean obtained from 5 cores is therefore uncertain by 22%. Comparing peaks
296 maximum induces a bias related to the sampling method: with a two centimeters resolution on average,
297 peak's height is directly impacted by the cutting, which tends to smooth the maxima. Comparing the
298 total sulfate deposited during the event is more appropriate. Proceeding on a similar approach, but
299 reasoning on mass of deposited sulfate rather than maximum concentration (and considering $F_i/F_{mean}$,
300 $F_i$ being the mass flux of peak i), the obtained variability is higher than previously. The uncertainty on
301 the flux for one measurement is 65 % (based on the standard deviation of the mean), and the
302 uncertainty of the mean (standard error of the mean) is therefore close to 30%. The difference in the
303 signal dispersion between the two approaches rests on the fact that peak maximum has a tendency to
304 smooth the concentration profile as a consequence of the sampling strategy. This artifact is suppressed
305 when the total mass deposited is considered.
306
307 **Conclusion:**
308 This study confirms in many ways previous work on multiple drilling variability [*Wolff et al.*, 2005].
309 As already discussed, peaks flux uncertainty can be significantly reduced (65 % to 29 %) by averaging
310 5 ice-cores signals. A 5-cores composite profile has been built using the criteria that a peak is
311 considered as volcanic if present at least in two cores. We observed that the number of volcanic peaks
312 listed in a composite profile increases with the number of cores considered. With 2 cores, only 33 %
313 of the peaks present in the composite profile are tagged as volcanoes. This percentage increases to
314 68 % with 5 cores. However, we did not observe an asymptotic value, even with 5 cores drilled. A
315 record based on a single record in a low accumulation site is therefore very unlikely to be a robust
316 volcanic record. Of course, peaks presenting the largest flux are more likely to be detected in any
317 drilling, but the example of the Tambora shows that surface topography is variable enough to erase
318 even the most significant signal, although rarely. This variability in snow surface is evidenced in the
319 depth offset between two cores drilled less than 5 meters from each other, as peaks can easily be

situated 40 cm apart.

In low accumulation sites such as Dome C, where surface roughness can be on the order of the snow accumulation and highly variable, indices based on chemical records should be considered with respect to the time-scale of the proxy studied. Large time-scale trends are faintly sensitive to this effect. On the contrary, a study on episodic events like volcanic eruptions or biomass burning, with a deposition time in the order of magnitude of the surface variability scale should be based on a multiple-drilling analysis. A network of several cores is needed to obtain a representative record, at least in terms of recorded events. However, although lowered by the number of cores, the flux remains highly variable, and the mean flux obtained from 5 cores is still uncertain almost 30%. This point is particularly critical in volcanic reconstructions that rely on the deposited flux to estimate the mass of aerosols loaded in the stratosphere, and to a larger extent, the climatic forcing induced. Recent reconstructions largely take into account flux variability associated with regional pattern of deposition, but this study underlines the necessity of not neglecting local scale variability in low accumulation sites. Less variability is expected with higher accumulation rate, but this still has to be demonstrated. Sulfate flux is clearly one of the indicators of the eruption strength, but due to transport, deposition and post-deposition effects, such direct link should not be taken for granted.

With such statistical analysis performed systematically at other sites, we should be able to reveal even the smallest imprinted volcanoes in ice cores, extending the absolute ice core dating, the teleconnection between climate and volcanic events and improving the time-resolution of mass balance calculation of ice sheets.

## Acknowledgments

Part of this work would not have been possible without the technical support from the C2FN (French National Center for Coring and Drilling, handled by INSU. Financial supports were provided by LEFE-IMAGO, a scientific program of the Institut National des Sciences de l'Univers (INSU/CNRS), the Agence Nationale de la Recherche (ANR) via contract NT09-431976- VOLSOL and by a grant from Labex OSUG@2020 (Investissements d'avenir – ANR10 LABX56). E. G. deeply thanks the Fulbright commission for providing the PhD Fulbright fellowship. The Institute Polaire Paul-Emile Victor (IPEV) supported the research and polar logistics through the program SUNITEDC No. 1011. We would also like to thank all the field team members present during the VOLSOL campaign and who help us. Data are available at the World Data Center for paleoclimatology (http://www.ncdc.noaa.gov/paleo/wdc-paleo.html).

## References

Baroni, M., J. Savarino, J. Cole-Dai, V. K. Rai, and M. H. Thiemens (2008), Anomalous sulfur isotope compositions of volcanic sulfate over the last millennium in Antarctic ice cores, *J Geophys Res*, *113*(D20), D20112, doi: 10.1029/2008jd010185.

Barnes, P. R. F., E. W. Wolff, and R. Mulvaney (2006), A 44 kyr paleoroughness record of the Antarctic surface, J. Geophys. Res., 111, D03102, doi:10.1029/2005JD006349.

Bay, R. C., R. A. Rohde, P. B. Price, and N. E. Bramall (2010), South Pole paleowind from automated synthesis of ice core records, J. Geophys. Res.-Atmos., 115, doi:10.1029/2009jd013741.

Castellano, E., S. Becagli, M. Hansson, M. Hutterli, J. R. Petit, M. R. Rampino, M. Severi, J. P. Steffensen, R. Traversi, and R. Udisti (2005), Holocene volcanic history as recorded in the sulfate

368 stratigraphy of the European Project for Ice Coring in Antarctica Dome C (EDC96) ice core, *J*
369 *Geophys Res*, *110*(D6), D06114, doi: 10.1029/2004jd005259.
370 Crowley, T. J., and M. B. Unterman (2013), Technical details concerning development of a 1200 yr
371 proxy index for global volcanism, *Earth Syst. Sci. Data*, *5*(1), 187-197, doi: 10.5194/essd-5-187-2013.
372 Delmas, R. J., S. Kirchner, J. M. Palais, and J. R. Petit (1992), 1000 years of explosive volcanism
373 recorded at the South-Pole, *Tellus Ser. B-Chem. Phys. Meteorol.*, *44*(4), 335-350.
374 EPICA-community-members (2004), Eight glacial cycles from an Antarctic ice core, *Nature*, *429*,
375 623-628, doi: 10.1038/nature02599.
376 Gao, C., A. Robock, and C. Ammann (2008), Volcanic forcing of climate over the past 1500 years: An
377 improved ice core-based index for climate models, *J Geophys Res*, *113*(D23), D23111, doi:
378 10.1029/2008jd010239.
379 Gao, C., L. Oman, A. Robock, and G. L. Stenchikov (2007), Atmospheric volcanic loading derived
380 from bipolar ice cores: Accounting for the spatial distribution of volcanic deposition, *J Geophys Res*,
381 *112*(D9), D09109, doi: 10.1029/2006jd007461.
382 Gleckler, P. J., K. AchutaRao, J. M. Gregory, B. D. Santer, K. E. Taylor, and T. M. L. Wigley (2006),
383 Krakatoa lives: The effect of volcanic eruptions on ocean heat content and thermal expansion,
384 *Geophys Res Lett*, *33*(17), L17702, doi: 10.1029/2006gl026771.
385 Hammer, C. U. (1977), Past Volcanism Revealed by Greenland Ice Sheet Impurities, *Nature*,
386 *270*(5637), 482-486.
387 Jouzel, J. (2013), A brief history of ice core science over the last 50 yr, *Climate of the Past*, *9*(6),
388 2525-2547, doi: 10.5194/cp-9-2525-2013.
389 Kiehl, J. T., and B. P. Briegleb (1993), The Relative Roles of Sulfate Aerosols and Greenhouse Gases
390 in Climate Forcing, *Science*, *260*(5106), 311-314, doi: 10.1126/science.260.5106.311.
391 Langway, C. C., H. B. Clausen, and C. U. Hammer (1988), An inter-hemispheric volcanic time-
392 marker in ice cores from Greenland and Antarctica, *Annals of Glaciology*, *10*, 102-108.
393 Libois, Q., G. Picard, L. Arnaud, S. Morin, and E. Brun (2014), Modeling the impact of snow drift on
394 the decameter-scale variability of snow properties on the Antarctic Plateau, *Journal of Geophysical*

395 *Research: Atmospheres*, *119*(20), 11,662-611,681, doi: 10.1002/2014jd022361.
396 Lorius, C., J. Jouzel, C. Ritz, L. Merlivat, N. I. Barkov, Y. S. Korotkevich, and V. M. Kotlyakov
397 (1985), A 150,000-year climatic record from Antarctic ice, *Nature*, *316*(6029), 591-596, doi:
398 10.1038/316591a0.
399 Miller, G. H., Geirsdóttir, Á., Zhong, Y., Larsen, D. J., Otto-Bliesner, B. L., Holland, M. M., Bailey,
400 D. a., Refsnider, K. a., Lehman, S. J., Southon, J. R., Anderson, C., Björnsson, H. and Thordarson, T.
401 (2012), Abrupt onset of the Little Ice Age triggered by volcanism and sustained by sea-ice/ocean
402 feedbacks, *Geophys. Res. Lett.*, *39*(2), L02708, doi: 10.1029/2011gl050168.
403 Ortega, P., F. Lehner, D. Swingedouw, V. Masson-Delmotte, C. C. Raible, M. Casado, and P. Yiou
404 (2015), A model-tested North Atlantic Oscillation reconstruction for the past millennium, *Nature*,
405 *523*(7558), 71-74, doi: 10.1038/nature14518.
406 Parrenin, F., Barnola, J.-M., Beer, J., Blunier, T., Castellano, E., Chappellaz, J., Dreyfus, G., Fischer,
407 H., Fujita, S., Jouzel, J., Kawamura, K., Lemieux-Dudon, B., Loulergue, L., Masson-Delmotte, V.,
408 Narcisi, B., Petit, J.-R., Raisbeck, G., Raynaud, D., Ruth, U., Schwander, J., Severi, M., Spahni, R.,
409 Steffensen, J. P., Svensson, a., Udisti, R., Waelbroeck, C. and Wolff, E. W. (2007), The EDC3
410 chronology for the EPICA dome C ice core, *Climate of the Past*, *3*(3), 485-497, doi: 10.5194/cp-3-
411 485-2007.
412 Pfeiffer, M. A., B. Langmann, and H. F. Graf (2006), Atmospheric transport and deposition of
413 Indonesian volcanic emissions, *Atmos Chem Phys*, *6*, 2525-2537, doi:10.5194/acp-6-2525-2006.
414 Rampino, M. R., and S. Self (1982), Historic eruptions of Tambora (1815), Krakatau (1883), and
415 Agung (1963), their stratospheric aerosols, and climatic impact, *Quat. Res.*, *18*(2), 127-143, doi:
416 10.1016/0033-5894(82)90065-5.
417 Robock, A. (2000), Volcanic eruptions and climate, *Reviews of Geophysics*, *38*(2), 191-219.
418 Savarino, J., A. Romero, J. Cole-Dai, S. Bekki, and M. H. Thiemens (2003), UV induced mass-
419 independent sulfur isotope fractionation in stratospheric volcanic sulfate, *Geophys Res Lett*, *30*(21),
420 2131, doi: 10.1029/2003gl018134.
421 Severi, M., Becagli, S., Castellano, E., Morganti, a., Traversi, R., Udisti, R., Ruth, U., Fischer, H.,

Huybrechts, P., Wolff, E. W., Parrenin, F., Kaufmann, P., Lambert, F. and Steffensen, J. P. (2007), Synchronisation of the EDML and EDC ice cores for the last 52 kyr by volcanic signature matching, *Clim. Past*, *3*(3), 367-374, doi: 10.5194/cp-3-367-2007.

Sigl, M., Mcconnell, J. R., Layman, L., Maselli, O., Mcgwire, K., Pasteris, D., Dahl-jensen, D., Steffensen, J. P., Vinther, B., Edwards, R., Mulvaney, R. and Kipfstuhl, S. (2013), A new bipolar ice core record of volcanism from WAIS Divide and NEEM and implications for climate forcing of the last 2000 years, *Journal of Geophysical Research: Atmospheres*, *118*(3), 1151-1169, doi: 10.1029/2012jd018603.

Sigl, M., Mcconnell, J. R., Toohey, M., Curran, M., Das, S. B., Edwards, R., Isaksson, E., Kawamura, K., Kipfstuhl, S., Krüger, K., Layman, L., Maselli, O. J., Motizuki, Y., Motoyama, H. and Pasteris, D. R. (2014), Insights from Antarctica on volcanic forcing during the Common Era, *Nature Clim. Change*, *4*(8), 693-697, doi: 10.1038/nclimate2293.

Sigl, M., Winstrup, M., McConnell, J. R., Welten, K. C., Plunkett, G., Ludlow, F., Büntgen, U., Caffee, M., Chellman, N., Dahl-Jensen, D., Fischer, H., Kipfstuhl, S., Kostick, C., Maselli, O. J., Mekhaldi, F., Mulvaney, R., Muscheler, R., Pasteris, D. R., Pilcher, J. R., Salzer, M., Schüpbach, S., Steffensen, J. P., Vinther, B. M. and Woodruff, T. E. (2015), Timing and climate forcing of volcanic eruptions for the past 2,500 years, *Nature*, doi: 10.1038/nature14565.

Stocker, T. F., D. Qin, G.-K. Plattner, M. Tignor, S. K. Allen, J. Boschung, A. Nauels, Y. Xia, B. V., and M. P. M. (2013), IPCC, 2013: The Physical Science Basis, Fifth Assessment Report of the Intergovernmental Panel on Climate Change, Intergovernmental Panel on Climate Change 2013, United Kingdom and New York, NY, USA.

Timmreck, C. (2012), Modeling the climatic effects of large explosive volcanic eruptions, *Wiley Interdiscip. Rev.-Clim. Chang.*, *3*(6), 545-564, doi: 10.1002/wcc.192.

Wolff, E. W., E. Cook, P. R. F. Barnes, and R. Mulvaney (2005), Signal variability in replicate ice cores, *Journal of Glaciology*, *51*(174), 462-468, doi: 10.3189/172756505781829197.

Zielinski, G. A. (1995), Stratospheric loading and optical depth estimates of explosive volcanism over the last 2100 years derived from the Greenland- Ice-Sheet-Project-2 ice core, *J Geophys Res*,

449 *100*(D10), 20937-20955.

450

451 **Table 1** – Tie points used to set the time scale and synchronize the cores. Volcanic events are
452 named "Ev x" if they are not assigned to a well-known eruption. Dating of the events is based
453 on *Sigl et al.*, [2015].

454

| Eruption | core 1 | core 2 | core 3 | core 4 | core 5 | date of deposition |
|---|---|---|---|---|---|---|
| Surface | 0 | 0 | 0 | 0 | 0 | 2010 |
| Pinatubo | 1.53 | | | | | **1992** |
| Krakatoa | 8.82 | 8.92 | 8.67 | 8.71 | 8.63 | 1884 |
| Cosiguina | 11.98 | 11.83 | 11.65 | 11.62 | 11.46 | 1835 |
| Tambora | 12.85 | | | 12.6 | 12.57 | **1816** |
| UE 1809 | 13.33 | 13.3 | 13.04 | 13.08 | 12.98 | **1809** |
| ev 7 | 15.98 | 15.93 | 15.66 | 15.67 | 15.52 | 1762 |
| Serua/UE | 19.29 | 19.22 | 18.93 | 18.94 | 18.78 | **1695** |
| Ev 10 | 21.87 | 21.74 | 21.53 | 21.48 | 21.4 | 1646 |
| kuwae | 30.18 | 30.04 | 29.92 | 29.85 | 29.73 | **1459** |
| ev 16 - A | 37.35 | 37.29 | 37.17 | 37.04 | 36.91 | 1286 |
| ev 16 - B | 37.77 | 37.77 | 37.62 | 37.52 | 37.4 | **1276** |
| ev 16 - C | 38.1 | 38.04 | | 37.78 | | 1271 |
| Samalas | 38.49 | 38.46 | 38.28 | 38.2 | 38.09 | **1259** |
| ev 17 | 39.59 | 39.56 | 39.46 | 39.36 | 39.2 | **1230** |
| ev 18 | 41.87 | 41.83 | 41.7 | 41.6 | 41.41 | **1172** |
| ev 22 | 50.26 | 50.3 | 50.2 | 50.11 | 49.87 | 9599 |
| ev 27 | 60.77 | 60.72 | 60.66 | | 60.27 | **684** |
| ev 31 | 65.72 | 65.74 | 65.68 | 65.6 | 65.25 | **541** |
| ev 35 | 76.06 | 76.13 | 76 | 75.94 | 75.64 | 235 |
| ev 46 | 90.42 | 90.53 | 90.36 | 90.41 | 89.95 | **-214** |
| ev 49 | 97.15 | 97.16 | 97.19 | 97.22 | 96.74 | **-426** |
| ev 51 | 100.16 | 100.19 | | 100.22 | 99.7 | -529 |

455

456

**Table 2** – Sulfate peak (maximum concentration, in $ng.g^{-1}$, and flux of volcanic sulfate deposited, in $kg.km^{-2}$) considered as volcanic eruptions based on the statistical analysis of the 5 cores. Flux is calculated by integrating the peak, using the density profile obtained during the logging process. Volcanic flux values are corrected from background sulfate (calculated separately for each sulfate peak). 0 stands for non-detected events in the cores. Agung (3.77m) and Pinatubo (1.52m) were not included in the statistical analysis because they were analyzed only in core one and thus are marked as not applicable (N/A). The estimation of the average volcanic flux takes into account undetected peaks, for which the flux is considered 0. The relative error on the flux (estimated as 10%) takes into account the IC measurement relative standard deviation (below 4% based on standards runs), the error on firn density (relative error estimated as 2%) and the error on samples time length (10%). The last column displays data obtained from Castellano *et al*. (2005), for identical volcanic peaks. For similar peaks Castellano's flux generally falls into the average flux + 40% uncertainty, sometimes exceeding this value.

| Peak depth (m) | date (year) | ***core 1*** | | ***core 2*** | | ***core 3*** | | ***core 4*** | | ***core 5*** | | ***average**** | | |
|---|---|---|---|---|---|---|---|---|---|---|---|---|---|---|
| | | $[SO_4^{2-}]$ ($ng.g^{-1}$) | Volcanic flux (kg / $km^2$) | $[SO_4^{2-}]$ ($ng.g^{-1}$) | Volcanic flux (kg / $km^2$) | $[SO_4^{2-}]$ ($ng.g^{-1}$) | Volcanic flux (kg / $km^2$) | $[SO_4^{2-}]$ ($ng.g^{-1}$) | Volcanic flux (kg / $km^2$) | $[SO_4^{2-}]$ ($ng.g^{-1}$) | Volcanic flux (kg / $km^2$) | $[SO_4^{2-}]$ ($ng.g^{-1}$) | Volcanic flux (kg / $km^2$) | *1σ (flux)* |
| 1.52 | 1992 | 188 | 5.0 | N/A | N/A | N/A | N/A | N/A | N/A | N/A | N/A | 188 | 5.0 | 0.5 |
| 3.77 | 1964 | 207 | 5 | N/A | N/A | N/A | N/A | N/A | N/A | N/A | N/A | N/A | N/A | N/A |
| 6.24 | 1929 | 0 | 0.0 | 164 | 1.3 | 0 | 0.0 | 132 | 1.1 | 0 | 0.0 | 148 | 0.5 | 0.0 |
| 8.59 | 1891 | 0 | 0.0 | 0 | 0.0 | 0 | 0.0 | 134 | 1.3 | 117 | 0.9 | 126 | 0.4 | 0.0 |
| 8.92 | 1885 | 232 | 8.1 | 262 | 8.8 | 236 | 10.5 | 240 | 10.2 | 216 | 7.7 | 237 | 9.1 | 0.9 |
| 11.83 | 1839 | 220 | 7.7 | 173 | 5.4 | 190 | 4.9 | 177 | 5.5 | 173 | 4.0 | 187 | 5.5 | 0.6 |
| 12.08 | 1834 | 0 | 0.0 | 0 | 0.0 | 144 | 2.5 | 0 | 0.0 | 137 | 1.3 | 140 | 0.8 | 0.1 |
| 12.91 | **1816** | 455 | 13.1 | 0 | 0.0 | 0 | 0.0 | 188 | 1.8 | 307 | 6.0 | 317 | 4.2 | 0.4 |
| 13.3 | **1809** | 436 | 16.6 | 291 | 10.5 | 392 | 12.7 | 408 | 16.3 | 461 | 13.4 | 398 | 13.9 | 1.4 |
| 15.93 | **1762** | 176 | 2.7 | 248 | 6.7 | 201 | 3.4 | 0 | 0.0 | 0 | 0.0 | 208 | 2.5 | 0.3 |
| 19.29 | **1695** | 287 | 13.4 | 0 | 0.0 | 168 | 9.2 | 194 | 7.3 | 0 | 0.0 | 217 | 6.0 | 0.6 |
| 20.3 | 1674 | 261 | 7.8 | 0 | 0.0 | 0 | 0.0 | 196 | 4.3 | 178 | 2.3 | 212 | 2.9 | 0.3 |
| 20.7 | 1666 | 0 | 0.0 | 0 | 0.0 | 0 | 0.0 | 123 | 1.6 | 149 | 2.4 | 136 | 0.8 | 0.1 |
| 21.74 | **1646** | 257 | 10.1 | 249 | 10.3 | 259 | 13.2 | 282 | 17.5 | 257 | 13.2 | 261 | 12.8 | 1.3 |
| 22.72 | 1625 | 181 | 4.8 | 146 | 2.7 | 141 | 2.9 | 0 | 0.0 | 0 | 0.0 | 156 | 2.1 | 0.2 |
| 23.77 | 1600 | 225 | 10.6 | 0 | 0.0 | 170 | 2.5 | 0 | 0.0 | 0 | 0.0 | 197 | 2.6 | 0.3 |
| 25.78 | 1557 | 144 | 2.1 | 0 | 0.0 | 0 | 0.0 | 148 | 2.2 | 0 | 0.0 | 146 | 0.9 | 0.1 |
| 30 | **1459** | 496 | 33.2 | 442 | 31.1 | 422 | 31.6 | 543 | 37.2 | 559 | 36.9 | 493 | 34.0 | 3.4 |
| 30.56 | 1449 | 0 | 0.0 | 143 | 1.8 | 131 | 2.8 | 0 | 0.0 | 0 | 0.0 | 137 | 0.9 | 0.1 |
| 31.83 | 1417 | 0 | 0.0 | 0 | 0.0 | 0 | 0.0 | 155 | 2.6 | 148 | 2.6 | 151 | 1.0 | 0.1 |
| 33.51 | 1377 | 0 | 0.0 | 0 | 0.0 | 140 | 2.3 | 0 | 0.0 | 162 | 5.4 | 151 | 1.5 | 0.2 |
| 34.85 | 1348 | 273 | 12.4 | 288 | 14.2 | 209 | 7.9 | 303 | 18.3 | 269 | 13.2 | 268 | 13.2 | 1.3 |
| 37.29 | **1286** | 325 | 18.3 | 324 | 16.1 | 373 | 17.1 | 347 | 14.8 | 458 | 30.7 | 365 | 19.4 | 1.9 |
| 37.77 | **1276** | 563 | 28.9 | 605 | 40.4 | 570 | 28.8 | 525 | 26.3 | 497 | 21.6 | 552 | 29.2 | 2.9 |
| 38.04 | **1271** | 205 | 4.1 | 180 | 3.1 | 0 | 0.0 | 235 | 5.1 | 0 | 0.0 | 206 | 2.5 | 0.2 |

| | | | | | | | | | | | | | | |
|---|---|---|---|---|---|---|---|---|---|---|---|---|---|---|
| 38.46 | **1259** | 1086 | 59.7 | 1022 | 63.8 | 928 | 61.4 | 1030 | 78.5 | 1428 | 104.8 | 1099 | 73.6 | 7.4 |
| 39.25 | 1239 | 0 | 0.0 | 0 | 0.0 | 132 | 2.6 | 147 | 2.4 | 151 | 2.7 | 143 | 1.5 | 0.2 |
| 39.56 | **1230** | 268 | 17.8 | 260 | 16.8 | 279 | 15.6 | 315 | 18.7 | 320 | 16.7 | 288 | 17.1 | 1.7 |
| 41.17 | 1191 | 0 | 0.0 | 216 | 4.2 | 247 | 12.9 | 0 | 0.0 | 241 | 7.3 | 235 | 4.9 | 0.5 |
| 41.83 | **1172** | 437 | 30.9 | 401 | 29.4 | 377 | 25.2 | 378 | 23.3 | 433 | 29.4 | 405 | 27.6 | 2.8 |
| 44.4 | 1111 | 186 | 5.3 | 0 | 0.0 | 243 | 5.4 | 225 | 9.7 | 195 | 6.2 | 212 | 5.3 | 0.5 |
| 44.87 | 1099 | 174 | 2.5 | 0 | 0.0 | 0 | 0.0 | 153 | 2.4 | 0 | 0.0 | 163 | 1.0 | 0.1 |
| 45.81 | 1075 | 129 | 1.6 | 144 | 2.3 | 0 | 0.0 | 0 | 0.0 | 0 | 0.0 | 137 | 0.8 | 0.1 |
| 47.15 | 1041 | 187 | 3.6 | 193 | 3.6 | 217 | 4.4 | 0 | 0.0 | 203 | 6.2 | 200 | 3.6 | 0.4 |
| 47.5 | 1031 | 192 | 7.0 | 163 | 5.0 | 166 | 3.1 | 0 | 0.0 | 198 | 4.5 | 180 | 3.9 | 0.4 |
| 48 | 1018 | 0 | 0.0 | 155 | 3.2 | 168 | 2.8 | 0 | 0.0 | 0 | 0.0 | 161 | 1.2 | 0.1 |
| 49.63 | 976 | 132 | 2.0 | 0 | 0.0 | 139 | 2.5 | 0 | 0.0 | 0 | 0.0 | 135 | 0.9 | 0.1 |
| 50.3 | **959** | 209 | 8.2 | 256 | 15.6 | 236 | 12.6 | 220 | 11.9 | 227 | 12.1 | 230 | 12.1 | 1.2 |
| 52.49 | 902 | 254 | 3.9 | 0 | 0.0 | 215 | 4.8 | 184 | 5.9 | 233 | 7.7 | 222 | 4.5 | 0.4 |
| 54.35 | 852 | 0 | 0.0 | 0 | 0.0 | 0 | 0.0 | 155 | 2.3 | 249 | 5.2 | 202 | 1.5 | 0.1 |
| 55.65 | 819 | 184 | 8.8 | 193 | 7.3 | 191 | 6.7 | 181 | 7.1 | 249 | 5.2 | 200 | 7.0 | 0.7 |
| 58.26 | 749 | 155 | 3.2 | 202 | 3.4 | 0 | 0.0 | 201 | 6.6 | 0 | 0.0 | 186 | 2.6 | 0.3 |
| 60.72 | **684** | 287 | 12.9 | 216 | 14.0 | 243 | 7.8 | 0 | 0.0 | 230 | 4.9 | 244 | 7.9 | 0.8 |
| 64.49 | 577 | 528 | 36.0 | 0 | 0.0 | 430 | 25.8 | 367 | 21.4 | 393 | 23.3 | 430 | 21.3 | 2.1 |
| 65.74 | **541** | 287 | 19.1 | 274 | 12.7 | 283 | 20.5 | 306 | 21.5 | 304 | 16.3 | 291 | 18.0 | 1.8 |
| 68.41 | 465 | 132 | 2.9 | 0 | 0.0 | 182 | 4.4 | 0 | 0.0 | 0 | 0.0 | 157 | 1.5 | 0.1 |
| 69.41 | 436 | 194 | 10.7 | 168 | 3.8 | 0 | 0.0 | 207 | 11.1 | 233 | 9.1 | 201 | 7.0 | 0.7 |
| 72.38 | 352 | 0 | 0.0 | 172 | 4.7 | 203 | 5.3 | 0 | 0.0 | 188 | 5.8 | 188 | 3.2 | 0.3 |
| 73.13 | 331 | 0 | 0.0 | 169 | 4.1 | 152 | 2.8 | 0 | 0.0 | 0 | 0.0 | 160 | 1.4 | 0.1 |
| 73.95 | 304 | 0 | 0.0 | 0 | 0.0 | 171 | 3.7 | 190 | 5.7 | 0 | 0.0 | 180 | 1.9 | 0.2 |
| 76.13 | **235** | 205 | 12.1 | 258 | 20.0 | 237 | 21.7 | 287 | 23.8 | 262 | 13.0 | 250 | 18.1 | 1.8 |
| 77.17 | 206 | 179 | 5.4 | 206 | 15.4 | 211 | 12.5 | 219 | 13.2 | 272 | 13.5 | 217 | 12.0 | 1.2 |
| 78.31 | 172 | 250 | 15.3 | 0 | 0.0 | 156 | 4.3 | 203 | 5.4 | 219 | 7.7 | 207 | 6.6 | 0.7 |
| 79.98 | 125 | 165 | 4.4 | 187 | 3.7 | 0 | 0.0 | 162 | 3.2 | 167 | 3.3 | 170 | 2.9 | 0.3 |
| 84.5 | -4 | 202 | 9.8 | 199 | 7.7 | 222 | 5.0 | 0 | 0.0 | 188 | 7.9 | 203 | 6.1 | 0.6 |
| 85.44 | -37 | 0 | 0.0 | 155 | 4.4 | 0 | 0.0 | 0 | 0.0 | 240 | 8.6 | 197 | 2.6 | 0.3 |
| 87.89 | -128 | 236 | 11.2 | 212 | 9.6 | 270 | 12.9 | 244 | 12.1 | 0 | 0.0 | 241 | 9.1 | 0.9 |
| 89.28 | -173 | 0 | 0.0 | 0 | 0.0 | 0 | 0.0 | 190 | 5.6 | 164 | 3.7 | 177 | 1.9 | 0.2 |
| 90.53 | **-214** | 276 | 18.8 | 286 | 26.1 | 278 | 16.5 | 296 | 18.1 | 241 | 6.9 | 275 | 17.3 | 1.7 |
| 91.72 | -251 | 0 | 0.0 | 0 | 0.0 | 0 | 0.0 | 227 | 10.4 | 244 | 12.5 | 236 | 4.6 | 0.5 |
| 94.83 | -347 | 0 | 0.0 | 191 | 4.6 | 198 | 5.9 | 216 | 8.7 | 0 | 0.0 | 201 | 3.8 | 0.4 |
| 97.16 | **-426** | 331 | 22.6 | 228 | 15.4 | 403 | 35.2 | 436 | 48.5 | 675 | 75.0 | 414 | 39.3 | 3.9 |
| 97.31 | -431 | 0 | 0.0 | 131 | 2.9 | 0 | 0.0 | 0 | 0.0 | 0 | 0.0 | 65 | 0.6 | 0.1 |
| 100.19 | **-529** | 219 | 12.1 | 224 | 6.6 | 0 | 0.0 | 247 | 15.9 | 235 | 7.7 | 231 | 8.5 | 0.8 |

**Table 3** – Statistics on sulfate signal for identical peaks in core 1, 2, 3, 4 and 5. Geometric standard deviations are calculated on peaks heights (i.e maximum concentration reached, in $ng.g^{-1}$) and on peaks sulfate flux (i.e total mass of volcanic sulfate deposited after the eruption). Background corrections are based on background values calculated separately for each volcanic event.

| Study | Number of compared cores | Geom. std deviation based on maximum concentration | Geom std deviation based on deposition flux |
|---|---|---|---|
| Wolff and others | 2 | 1.5 | |
| This study | 5 | 1.49 | 1.65 |

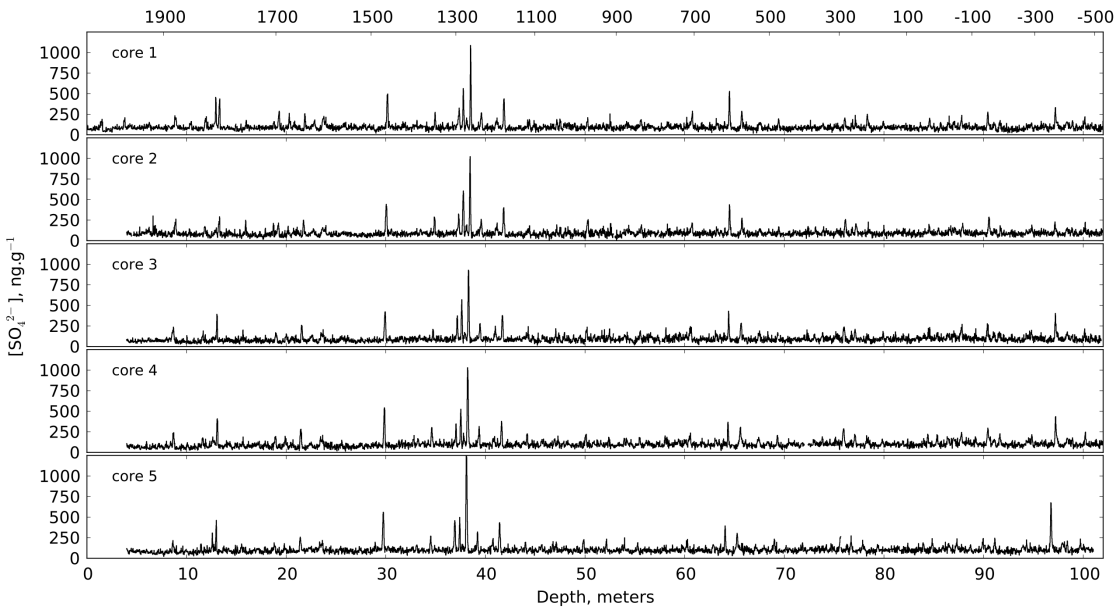


**Figure 1** - Sulfate profiles on the 5 replicate cores obtained during a drilling operation at Dome C – Antarctica in 2011.

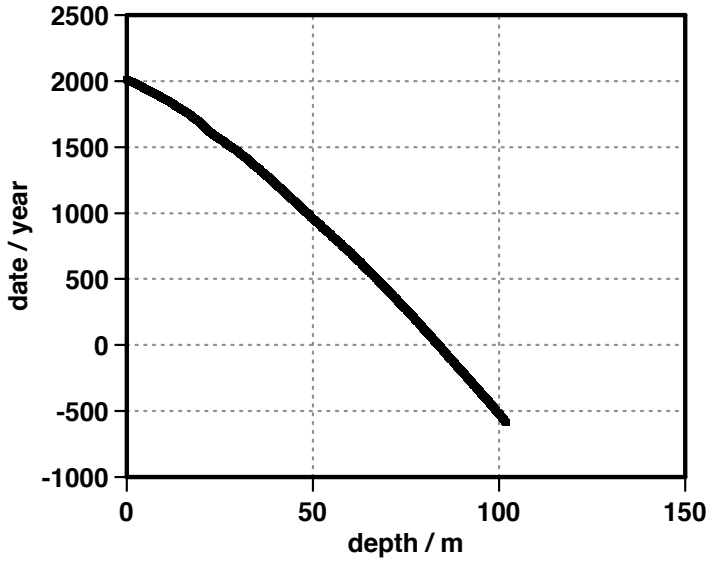


516
517
518

519 **Figure 2** - Age versus depth in core 1 drilled in 2011 CE, Dome C – Antarctica

520

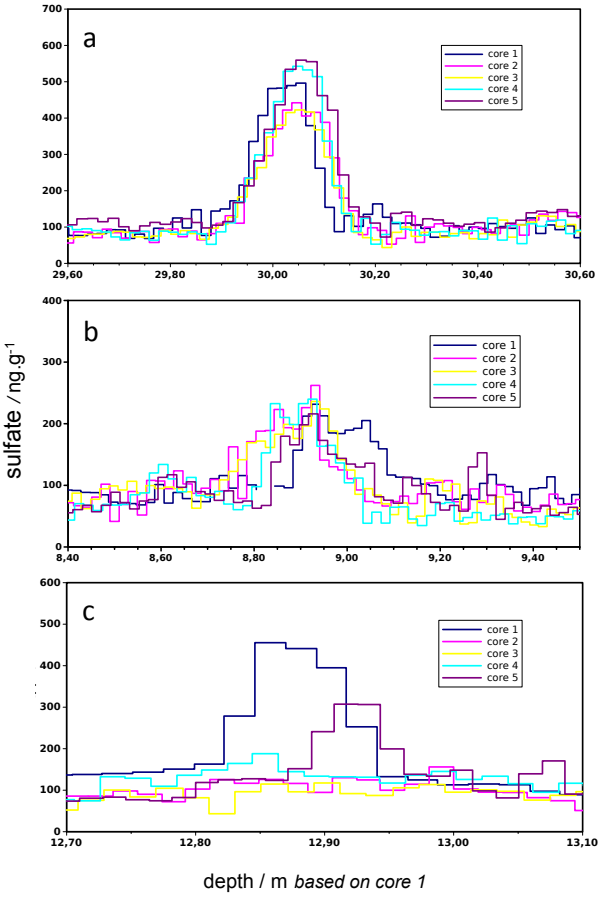


**Figure 3** –Kuwae (a, top), Krakatoa (b, middle) and Tambora (c, bottom) sulfate concentration profiles after depth synchronization. All peaks are within a 20 cm uncertainty, enabling to clearly attribute each occurrence to a single event.

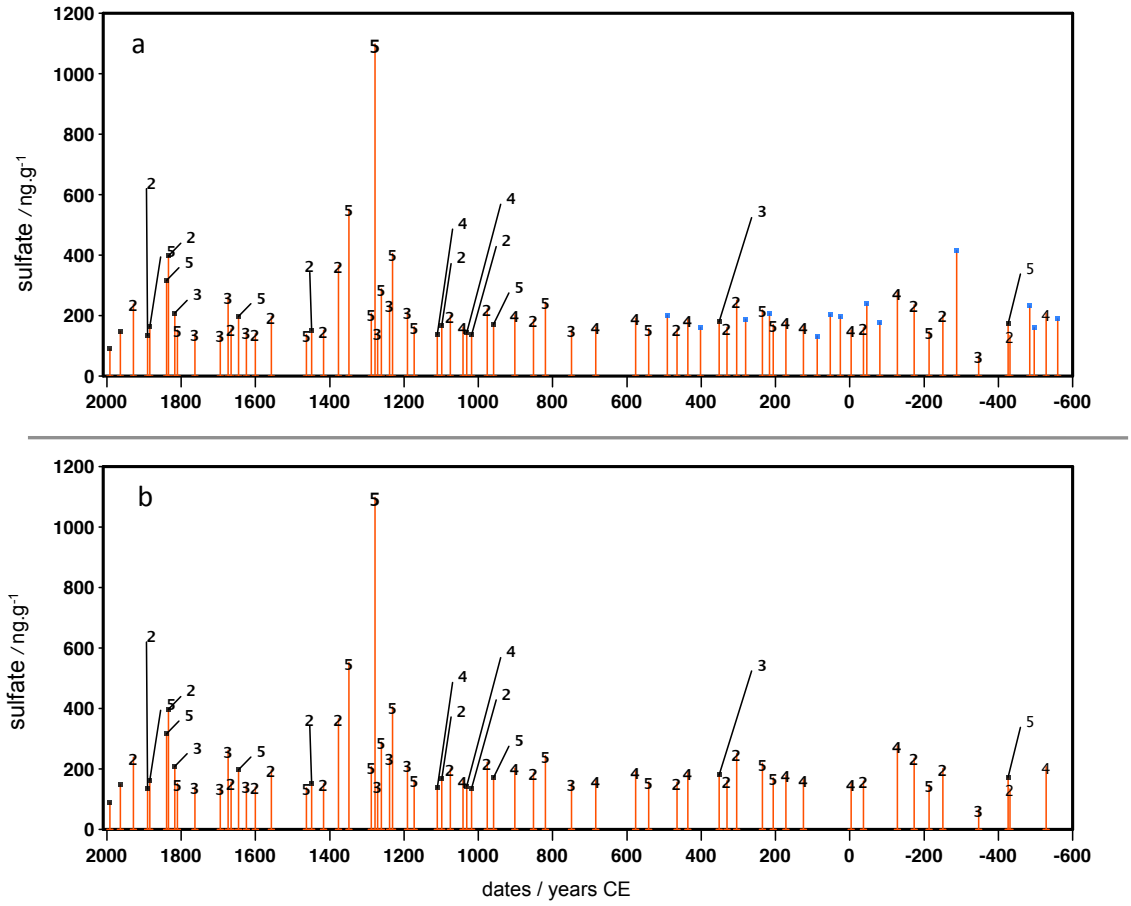


**Figure 4** – a) Composite sulfate peak profile deduced from our statistical analysis of the 5 cores using our detection peak and synchronization algorithms (see text). The numbers indicate the number of time a common peak is found in the cores. Unnumbered peaks, peaks found only in single core. b) same as a) without the single detected peaks. All the remaining peaks are considered as volcanic eruptions. See Table 2 for details.

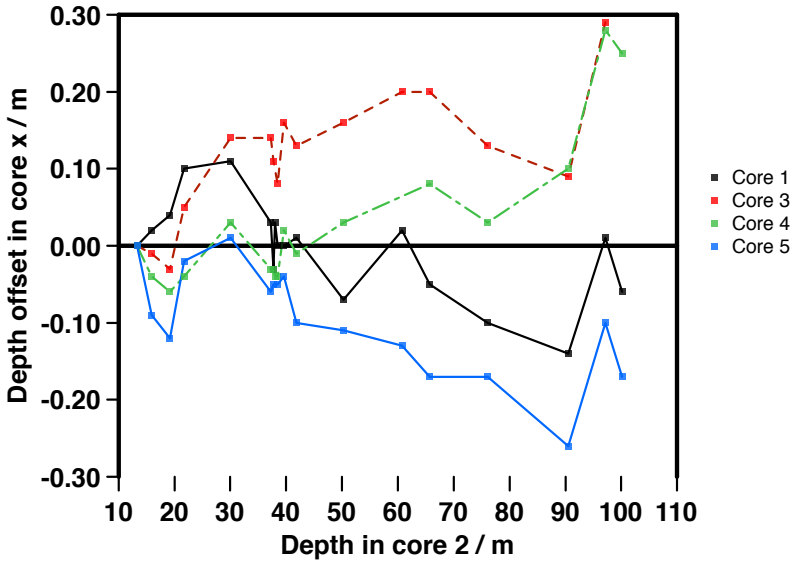


545
546

547 **Figure 5** – Depth offset of 18 common and well-identified volcanic events in cores 1, 3, 4 and

548 5 relatively to core 2. To overcome offset due to the drilling process and poor core quality on

549 the first meters, UE 1809 (depth ca. 13 m) is taken as the origin and horizon reference.

550

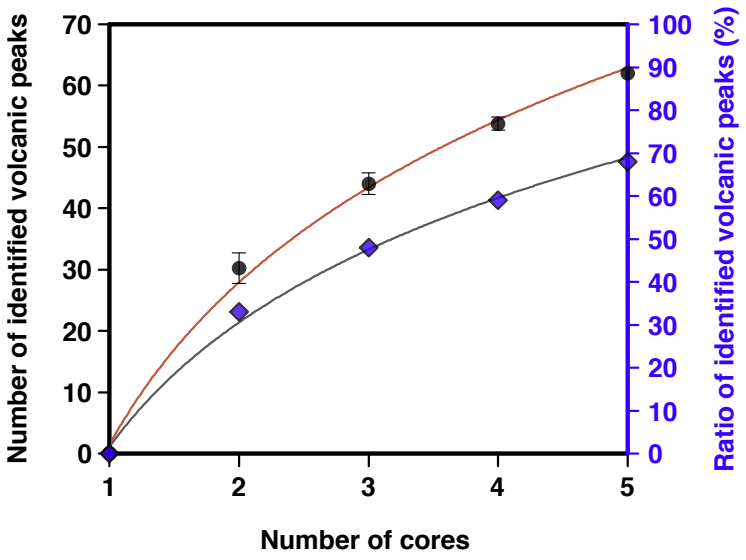


**Figure 6 –** Black dots with red line (left axis) represent the number of sulfate peaks that can be identified as volcanic peaks in a composite profile, made of n cores (with n ranging from 1 to 5). A sulfate peak appearing simultaneously in at least two cores is considered to be a volcanic peak. Blue diamonds represent the ratio of identified volcanic peaks, i.e the number of identified volcanic peaks (plotted on the left axis), relatively to the total number of sulfate peaks (no discrimination criteria) in a composite made of 5 cores. In our case, the 5 ice-cores composite comprises 91 sulfate peaks (Agung and Pinatubo excluded). With two cores, only 33% of them would be identified as being volcanic peaks (detected in both cores), while 68% of them can be identified as volcanic events using 5 cores.

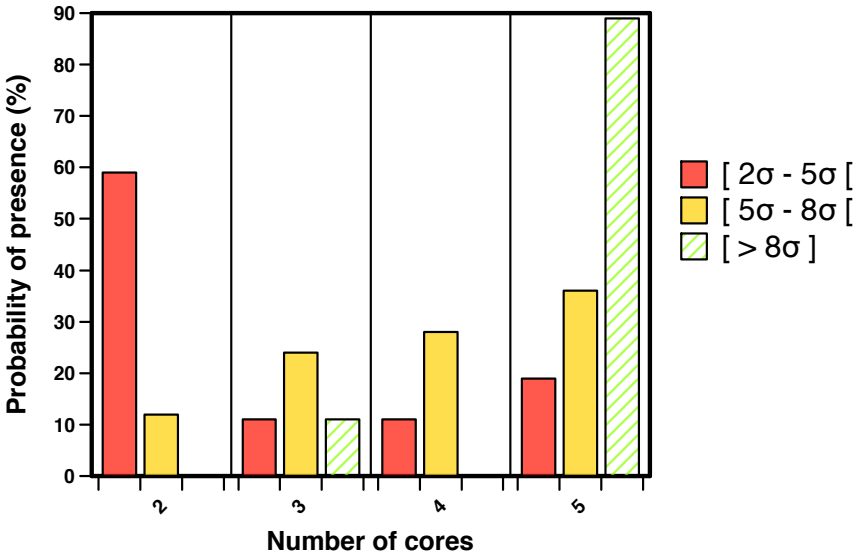


**Figure 7** - Peaks probability to be detected in 2, 3, 4 or 5 cores, as function of their flux. The three categories of flux are defined by peaks flux value, relatively to the average background flux, and quantified by x time (2, 5 and 8) the flux standard deviation (calculated for a 30 ppb standard deviation in concentrations). At flux above *background flux* + *8σ*, the volcanic peak has 90% chance to be detected in each core of a population of 5 cores. On the other hand, at flux below *background flux* + *5 σ*, the volcanic peak has a probability of 60% to be detected in 2 cores only, among the 5 cores population. This highlights that replicate cores are particularly useful to avoid missing small to intermediate peaks in a record.

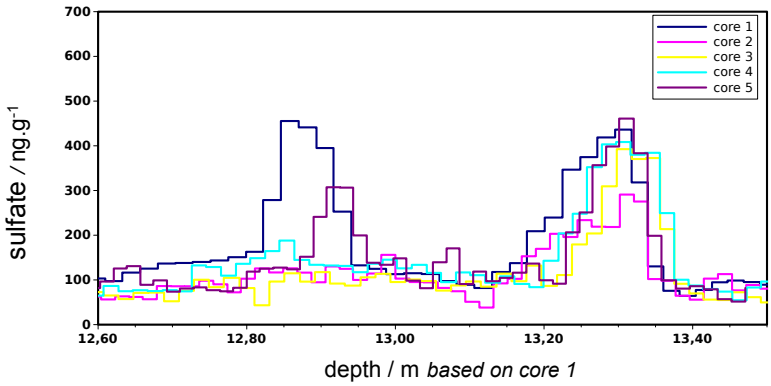


**Figure 8:** Close look at UE 1809 and Tambora (1815) events showing the absence of the Tambora event in 2 out of the 5 cores. This figure illustrates the possibility of missing major volcanic eruptions when a single core is used.

# SOM

1. Gfeller *et al*. (2014) method relies on calculating inter-series correlation (expressed as $R_{n,N}$, n being a subset of N time series). To calculate the representativeness of the mean of a given subset of cores, and by letting N going to infinity (simulating a fictive infinite number of cores), Gfeller *et al*. (2014) use the $\check{R}^2_{n,\infty}$ proxy. We used the same proxy of sulfate representativeness on Dome C 5 cores and obtained the following results:

| n *(number of cores)* | 1 | 2 | 3 | 4 | 5 |
|---|---|---|---|---|---|
| $\check{R}^2_{n,\infty}$ $SO_4^{2-}$ | **0.72** | **0.84** | **0.89** | **0.91** | **0.93** |

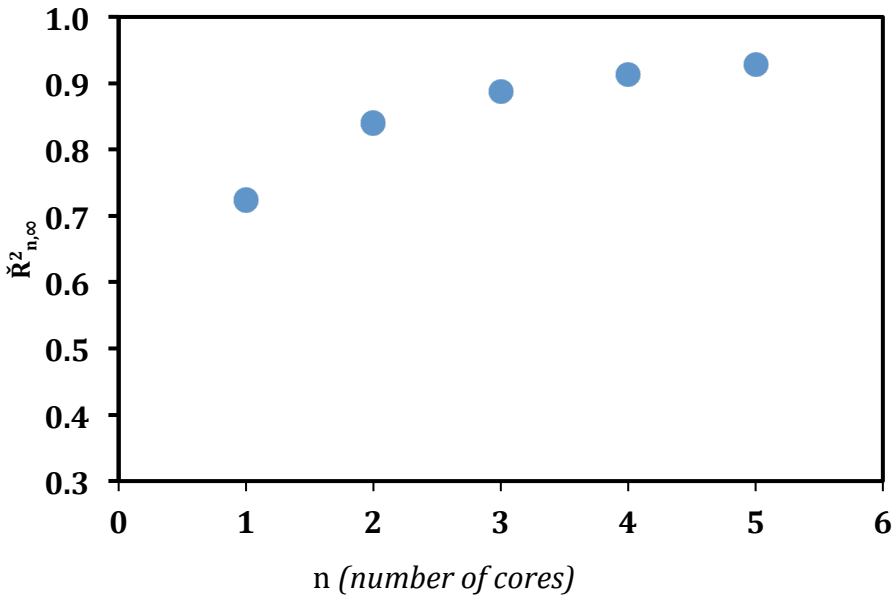


Figure S1: Representativeness of sulfate in the cores ($\check{R}^2_{n,\infty}$ ) as a function on the number of cores n (based on Gfeller et al., 2014 approach).

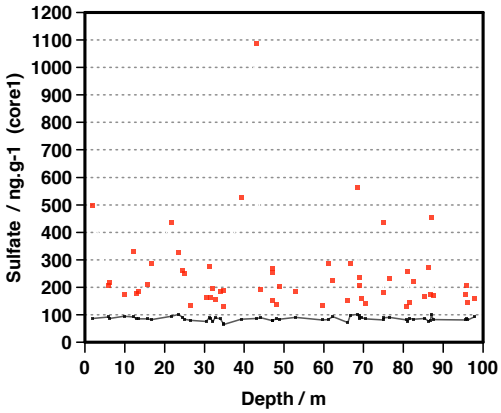


Figure S2 - Variation of the background along depth in core 1, red dots are detected peaks, the dark line stands for the background concentration.